Enhanced Marine Predators Algorithm for identifying static and dynamic Photovoltaic models parameters

Mohamed Abd Elaziz[a,b], Thanikanti Sudhakar Babu[c], Ibrahim Anwar Ibrahim[d,e], Songfeng Lu[a], Benedetto Nastasi[f], Majed A. Alotaibi[g], Md Alamgir Hossain[h], Dalia Yousri[i]

[a]*Hubei Engineering Research Center on Big Data Security, School of Cyber Science and Engineering, Huazhong university of Science and Technology, Wuhan 430074, China*
[b]*Department of Mathematics, Faculty of Science, Zagazig University, Zagazig 44519, Egypt*
[c]*Department of Electrical and Electronics Engineering, Chaitanya Bharathi Institute of Technology, Hyderabad, 500075, India.*
[d]*School of Engineering, Macquarie University, Sydney, NSW 2109, Australia.*
[e]*CSIRO Energy, 10 Murray Dwyer Cct, Mayfield West, NSW 2300, Australia.*
[f]*Department of Planning, Design and Technology of Architecture, Sapienza University of Rome, Via Flaminia 72, 00196, Rome, Italy*
[g]*Department of Electrical Engineering, College of Engineering, King Saud University, Riyadh 11421, Saudi Arabia.*
[h]*Capability Systems Centre (SEIT), The University of New South Wales-Canberra, ACT 2612, Australia.*
[i]*Electrical Engineering Dept., Faculty of Engineering, Fayoum University, Fayoum, Egypt.*
abd_el_aziz_m@yahoo.com, sudhakarbabu@ieee.org, ibrahim.a.ibrahim@hdr.mq.edu.au, lusongfeng@hust.edu.cn, benedetto.nastasi@outlook.com, majedalotaibi@ksu.edu.sa, md.hossain6@unsw.edu.au, day01@fayoum.edu.eg

Abstract

Providing an accurate and precise photovoltaic model is a vital stage prior to the system design, therefore, this paper proposes a novel algorithm, enhanced marine predators algorithm (EMPA), to identify the unknown parameters for different photovoltaic (PV) models including the static PV models (single-diode and double-diode) and dynamic PV model. In the proposed EMPA, the differential evolution operator (DE) is incorporated into the original marine predators algorithm (MPA) to achieve stable, and reliable performance while handling that nonlinear optimization problem of PV modeling. Three different real datasets are used to show the effectiveness of the proposed algorithm. In the first case study, the proposed algorithm is used to identify the unknown parameters of a single-diode and double-diode PV models. The root-mean-square error (RMSE) and standard deviation (STD) values for a single-diode are $7.7301e^{-04}$ and $5.9135e^{-07}$. Similarly for double diode are $7.4396e^{-04}$ and $3.1849e^{-05}$, respectively. In addition, the second case study is used to test the proposed model in identifying the unknown parameters of a double-diode PV model. Here, the proposed algorithm is compared with classical MPA in five scenarios at different operating conditions. In this case study, the RMSE and STD of the proposed algorithm are less than that obtained by the MPA algorithm. Moreover, the third case study is utilized to test the ability of the proposed model in identifying the parameters of a dynamic PV model. In this case study, the performance of the proposed algorithm is compared with the one obtained by MAP and heterogeneous comprehensive learning particle swarm optimization (HCLPSO) algorithms in terms of RMSE $\pm$ STD. The obtained value of RMSE $\pm$ STD by the proposed algorithm is $0.0084505 \pm 1.0971e-17$, which is too small compared with that obtained by MPA and HCLPSO algorithms ($0.0084505 \pm 9.6235e-14$ and $0.0084505 \pm 2.5235e-9$). The results show the proposed model's superiority over the MPA and other recent proposed algorithms in data fitting, convergence rate, stability, and consistency. Therefore, the proposed algorithm can be considered as a fast, feasible, and a reliable optimization algorithm to identify the unknown parameters in static and dynamic PV models.

*Corresponding author
Email address: sudhakarbabu66@gmail.com (Thanikanti Sudhakar Babu)

Keywords: solar energy technology, marine predator algorithm, parameters estimation, single diode model, two diode model.

Nomenclature

Acronyms

AE_{MPP} absolute error at maximum power point

ABC artificial bee colony

CPSO chaos particle swarm optimisation

CS cuckoo search

CWOA improved whale optimization algorithm variants

DC direct current

DC-DC direct current to direct current

DDM double diode PV model

DE differential evolution

DM dynamic model

EJADF improved differential algorithm

ELPSO enhanced leader particle swarm optimisation

EMPA enhanced marine predators algorithm

EPSO ensemble particle swarm optimizer

FADS fish aggregating devices

FOM fractional order dynamic PV model

GA genetic algorithm

GWOCS grey wolf optimizer and cuckoo search

HCLPSO heterogeneous comprehensive learning particle swarm optimization

HFAPS hybrid firefly and pattern search algorithms

HHO harris hawks optimization

I-T current - time

I-V current - voltage

ICSA improved cuckoo search algorithm

IOM integer order dynamic PV model

IWOA improved whale optimization algorithm

JAYA jaya algorithm

LB lower boundary

MLBSA multiple learning backtracking search algorithm

MPA marine predators algorithm

MRFO manta ray foraging optimization

MSAE mean sum absolute error

NR newton-Raphson

P-N positive-negative

PGJAYA performance-guided JAYA

PSO particle swarm optimization

PV photovoltaic

RMSE root mean square error

$\text{RMSE}_{Lambert}$ RMSE calculated via Lambert W function

SCA sine cosine algorithm

SDM single diode PV model

SSA salp swarm algorithm

STD standard deviation

STLBO self-adaptive teaching-learning-based optimization

TLBO teaching learning based optimization

TVACPSO time varying acceleration coefficients particle swarm optimisation

TW terawatt

UB upper boundary

Variables

a_1, a_2 ideality factors of diodes D_1 and D_2

I_{01}, I_{02} leakage currents of diodes D_1 and D_2

$I_{Lambert}$ calculated current via Lambert form

R_p shunt resistance

R_s series resistance

1. Introduction

Sustainable power sources have acknowledged incredible concern worldwide because of different vital reasons, including the shortage of petroleum products and increasing their price moreover the atmospheric concerns that boots the inclination to have a green and healthy environment [1]. The photovoltaic (PV) has viewed as a financially economical renewable power technology in the short-term because of the high decrease in the cost of the PV components in the most recent decade [2]. The increase in the technological development in a solar PV system and awareness of using it towards moving into green energy may lead to rising the installation's capacity to 2.8 terawatts (TW) by 2030 that imitates the enormous production of PV modules into the market [2]. In light of that, the industries that produce large scale PV modules and supplies to the market require an extraordinary examination and accurate modeling. This leads to high research focusing on PV systems' dynamic impact under different irradiations and temperature conditions. Therefore, it indicates that the entire PV system performance depends on its effective modeling [3].

The PV module can be implemented via different equivalent circuits including four-parameter models also known as series resistance R_s model [4], five-parameter model (single-diode model (SDM)), a parallel resistance R_p model [5], or double-diode model (DDM) [6]. Whereas the strong nonlinear characteristic and an implicit in nature are the common features of those models. Besides, the necessary data required to model PV is not provided by the manufacturer. Therefore, PV modeling becomes a challenging task in the present condition [7]. Indeed, some research lines neglect the device modeling in assessing renewable energy production from the resources assessment [8**?**]. To beat these difficulties, a few researchers worked on utilizing nonlinear electrical models of solar cells to extricate its viable parameters [9, 10]. Concerning any physical system, the PV cell designing is constantly done with various degrees of accuracy. This assignment is reliably accomplished through an electrical equivalent circuit of the PV cell and utilizes its involved parameters [11].

The PV models studied in the literature so far, i.e., R_s model, SDM, and DDM, are considered static models. In these static PV models, the change in load conditions and switching states of DC-DC converter/inverter are failed to consider. However, in real-time conditions, the load may not always be constant. Moreover, resonance on DC cables, under-damped currents, and switching frequency harmonics are needed to be considered for accurate modeling. The developed PV model should also emulate the high frequency of large square wave signals [12]. With this motivation, the authors focused on developing dynamic PV models that are more efficient to tackle static models' limitations and work effectively with real-time conditions. The authors in [13] developed a dynamic PV model (DM) for the first time by considering the real operating scenarios. Chin et.al. [14] and Abdelaty et al. [15] proved that the dynamic PV model is more recommended for the application of grid-connected PV systems. Accordingly, either static or dynamic PV models' performance strongly depends on its effective modeling, and its high priority as the manufacturer does not provide the required parameters. Therefore, numerous streamlining algorithms have been utilized to extract the PV module's parameters, which can be ordered into three distinct families.

The first category is an analytical one where the problem can be solved by using mathematical equations. The techniques implemented using this approach are analytical extraction method [16], compound method [17], and another method based on key points of I-V curves were proposed in [18], to estimate PV parameters. The algebraic equations were solved by proposing a relationship between I-V curves of a considered PV model to identify PV parameters. This method had overcome the limitation of estimating MPP and open-circuit voltage. However, it has more complex in maintaining the relationship between I-V curves. Even though these techniques can acquire results rapidly and effectively, a few presumptions should be made ahead of time processing, which leads to inaccurate solutions. The analytical method also requires exact information of parameters such as short circuit current, open-circuit voltage, maximum power voltage, and current. Without this accurate information, the parameters' accurate extraction cannot be achieved [19, 16]. Therefore, the analytical methods are often uncertain and give unsatisfactory results in most cases [20]. Numerical methodologies use the single point information on the real I-V curve to precisely duplicate the I-V characteristics. Even though this methodology is extremely well known, it devours all the information that focuses on the I-V curve and confuses the computation [21, 22].

The second category of estimation of PV parameters is the deterministic approach. The more popular methods that fall under this approach are lambert W-functions [23], and the Newton-Raphson (NR) method [24]. However, the reliable local search capacity of those methods. It is sensitive to the initial solutions and simple to trap into local optimal points. Furthermore, those methods have complex considerations in the objective functions of the models like convexity and differentiability. Therefore, these drawbacks lead to model failure in most of the cases [25]. Therefore, the researchers motivated the third category to tackle the first and second categories' previously mentioned drawbacks.

The final category is the meta-heuristic based optimization techniques. These techniques have evolved due to their extensive features. These algorithms do not have any requirements for building objective function, easy to implement, a wide range of search behavior, and effectively solving different complex problems. They attract the researchers to consider these algorithms for the effective modeling of solar PV. With this motivation, the various optimization algorithms developed by researchers recently for the application of PV modeling are: (i) an improved particle swarm optimization (PSO) with adaptive mutation strategy was introduced in [26]; (ii) a performance-guided JAYA algorithm for different PV modules were presented in [27]; (iii) multiple learning backtracking search algorithm in [28]; (iv) a self-adaptive approach is incorporated into TLBO, and its improved algorithms for effective modeling of PV are proposed in [29, 30], by utilizing the effective features of JADE algorithm such as faster response, accuracy; (v) an improved differential algorithm (EJADF) is proposed for modeling of DDM in [31];(vi) Dalia et al., in [32, 33] proposed a PSO variant algorithm for static and dynamic PV parameter estimation. Metaphor-less algorithms [34] and Hasanien et. al., [35] enhanced the PV system performance by effective modeling via whale optimization technique. Xiong et al., in [36] introduced an improved whale optimization algorithm (IWOA) for three types of PV models. The proposed approach is successfully tested in PV power stations practically with a large number of PV modules. Hybrid TLBO and ABC are implemented in [37], another hybrid algorithm combining the features of the grey wolf and cuckoo search optimizer (GWOCS) is introduced in [20], Chen et al., in [38], introduced hybrid cuckoo search with a bio-geography-based optimization technique. Qais et al., in [39] by combining the analytical and optimization approach, introduced a new algorithm named sunflower optimization technique for the extraction of three diode model parameters. Using a guaranteed PSO technique, a new hybrid algorithm to enhance the performance of PV modeling is proposed in [40]. Fractional chaos maps have been utilized to enhance the ensemble particle swarm optimizer for single, double, and three diode models in [33]. A hybrid adaptive TLBO and DE for SDM is proposed in [41], Heuristic iterative method is proposed to estimate five parameters of SDM in [42]. This method is introduced to solve the implicit current and voltage equations simultaneously. The achieved results using this method shows high performance to the De Soto model and analytical techniques. Further, model parameters for PV arrays using reinforcement learning (RL) technique via on-line are proposed in [43]. The authors found that the RL technique can also combine with the online fault detection technique to estimate PV parameters concerning atmospheric conditions. To bring numerous meta-heuristic-based PV parameter estimation methods at one place, in this article [44], the authors presented a comprehensive review to understand the practical applicability, limitations, and advantages of various methods. Similarly, comparative analysis concerning DE and other meta-heuristics methods were presented in [45]. Multiswarm spiral leader particle swarm optimization (M-SLPSO) specific to SDM is introduced in [46]. The authors implement the marine predators algorithm to extract the triple diode model in [47]. Similarly, by observing the features of MPA algorithm, its improved version named comprehensive learning dynamic multi-swarm marine predators algorithm is proposed to estimate the parameters of solid oxide fuel cell [48].

Even if these algorithms gave satisfactory results, still, there is a chance to improve their convergence, consistency, and reliability. The proposed techniques still suffer from different limitations, such as the PSO method converges prematurely, and ABC exhibits indigent exploitation. CS effects with slow convergence. The effectiveness of DE depends on tunable parameters. Besides, these meta-heuristic algorithms' superiority should be fortified since the parameter extraction problem of PV models is a multi-modal streamlining issue. Therefore, producing an exact, reliable, and proficient meta-heuristic algorithm to estimate the unknown parameters and modeling PV is as yet continuous.

With these observations and motivation in this article, the authors proposed a simple and easiest algorithm with limited parameters. Recently, a marine predators algorithm (MPA) has been proposed by faramarzi et al., [49] to simulate the marine prey and predator's relation in nature. The MPA performance has been tested with numerous numerical benchmark functions, and it has shown its efficiency in comparison with several optimization algorithms. Moreover, the MPA's simplicity attracted Yousri et al., [50] to apply the MPA for large size PV array reconfiguration approach. The MPA confirmed its superiority in comparison with manta ray foraging optimization (MRFO), harris hawk optimizer (HHO), and particle swarm optimizer (PSO) in achieving the highest harvested PV power in the shortest execution time. Notwithstanding, the division of the iteration' numbers between the exploration and exploitation perspectives of the algorithm may cause trapping the search agents for the local solutions, especially while dealing with nonlinear and multi-modal optimization problems [48]. This observation motivated the authors to modify the MPA technique performance via merging the differential evolution optimizer in the exploration phase to ensure the agents' diversity to avoid the local solutions. As a result, an enhanced MPA (EMPA) has been developed to handle the nonlinear optimization problem of identifying the PV static models (single and double diode models) and dynamic PV model's parameters using several experimental measured data-sets under various environmental conditions. The following lines sum up the main contributions in the current work.

1. A novel optimization algorithm has been proposed for PV models parameters estimation based on MPA, and DE optimizer called enhanced MPA algorithm (EMPA).
2. The parameters of the static and dynamic PV models have been identified based on experimental data-sets with different environmental conditions.
3. The proposed algorithm has been compared with several state-of-the-art based on numerous statistical analyses.

The remaining sections of the article are organized as follows: The representation of static models with three different varieties (SDM, DDM PV modules) and dynamic PV model along with necessary equations and equivalent circuits are given in section 2. The problem formulation and detailed explanation on the development of objective function is conferred in section 3. Section 4 deals with the algorithms proposed for the application of static and dynamic PV parameter estimation. The detailed explaination and implementation steps of EMPA were detailed in section 5. The discussions on the obtained results of the carried-out work are presented in section 6, and an extensive sensitivity analysis is presented in section 7. Finally the outcome and observations of proposed work are concluded in section 8.

2. PV equivalent circuits

In this section, the details and equivalent electric circuit of the static and dynamic PV models have been addressed as below:

2.1. Static PV models

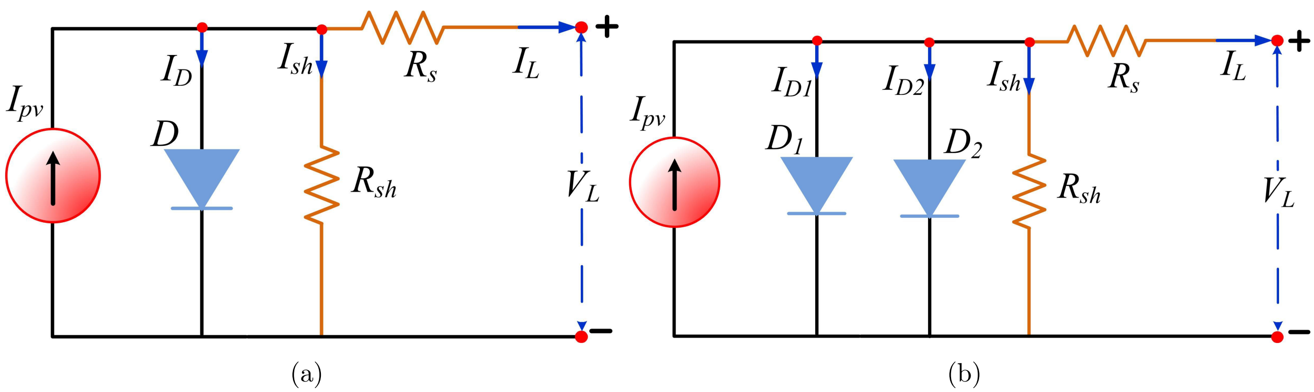

Figure 1: PV models (a) SDM, (b) DDM Topology.

PV cell could be named as a silicon diode with a P-N junction. The single diode model (SDM) is the most prominent in the practical applications because of the decent trade-off between the perfection of results produced and its simplicity [51]. The electrical equivalent circuit of SDM is shown in Fig. 1(a). This model comprises of photo-current source I_{pv} in parallel with diode D_1 and series and shunt resistance that are R_s and R_p, respectively. The R_s contemplates the impacts of silicon and surface contacts of electrodes, the resistance of electrodes and the current flowing through them. R_p intends to positive-negative (P-N) junction leakage current near to the edges of cells.

The current produced by SDM can be mathematically represented as in Eq.(1):

$$I_L = I_{pv} - I_{D1} - I_{sh} \tag{1}$$

where, I_{pv} is the photons current, I_{D1} is the diode current and the current flowing through shunt resistance can be given as I_{sh}. The diode current I_{D1} can be calculatedas given in Eq.(2):

$$I_{D1} = I_{01}\left(exp\left(\frac{V_L + I_L * R_s}{a_1 * V_T}\right) - 1\right) \tag{2}$$

where I_{01} is the reverse saturation current, a_1 is the ideality factor of D_1; I_L, V_L are the total current voltage generated by PV cell, R_s is the series resistance and V_T is the thermal voltage constant.

I_{sh} can be evaluated as given in Eq.(3):

$$I_{sh} = \frac{V + I * R_s}{R_{sh}} \tag{3}$$

V_T can be defined as $\frac{K_b * T}{q}$, K_b is Boltzmann's constant, q and T are electron's charge and absolute temperature.

From the presented equations of SDM, it can be understood that there exist five unknown parameters that need to be estimated for effective PV modeling. Namely, I_{01}, I_{pv}, R_s, R_p and a_1.

Another widely used type of PV model is the double diode. In this, an additional diode D_2 is connected anti-parallel to the PV current source. In this model, the recombination losses were taken into account. The additional diode signifies an additional current term in the output current equation of a PV model. The equivalent circuit of DDM is shown in Fig. 1(b). The current generated by DDM can be written as in Eqs. 4 and 5:

$$I_L = I_{pv} - I_{D1} - I_{D2} - I_{sh} \tag{4}$$

where, I_{D2} represents 2^{nd} diode D_2 current. It can be evaluated as given below:

$$I_{D2} = I_{02}\left(exp\left(\frac{V_L + I_L * R_s}{a_2 * V_T}\right) - 1\right) \tag{5}$$

where, I_{02} and a_2 are the reverse saturation current and ideality factor of diode D_2.

The number of parameters to be estimated for modeling of DDM are I_{01}, I_{02}, I_{pv}, R_s, R_p, a_1, and a_2. DDM comprises two additional parameters than SDM.

2.2. Dynamic model

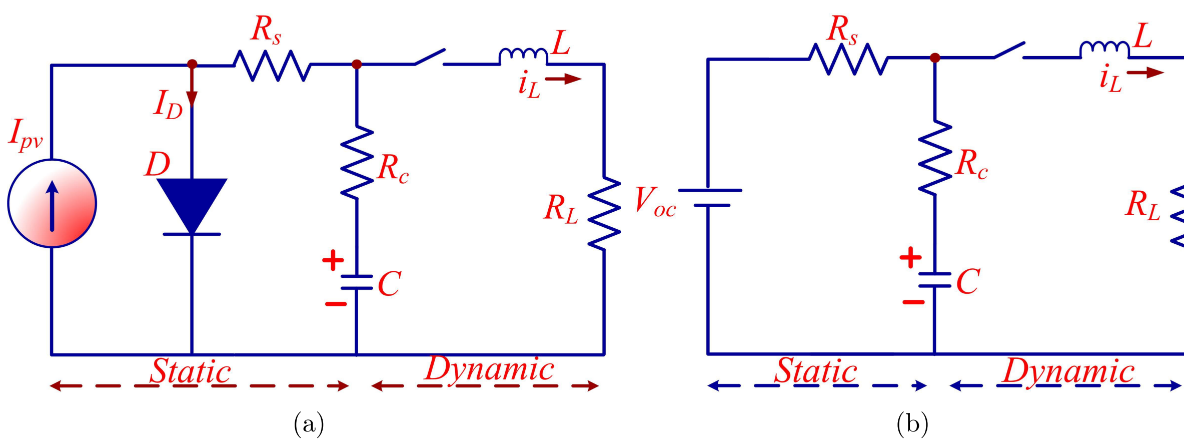

Figure 2: The dynamic PV model of (a) complete circuit, and (b) equivalent circuit.

Di Piazza et al. [13] proposed the dynamic PV model to consider the impact of the load fluctuations, and the switching circuits of converter/inverter in the PV model behaviour. The circuit of the dynamic PV model is shown in Fig. 2(a) where it comprises with static and dynamic parts. It can be observed from Fig. 2(a), that the static part which consists of source I_{pv} and diode D is minimized into a constant voltage source of V_{oc} and a series resistance R_s, as exhibited in Fig. 2(b). The other part of a PV model is a dynamic part, which includes a capacitor (C) represents junction capacitance, the conductance of the circuit is represents by (R_c) and a series inductance (L) is accounted for cabling inductance and connections.

To investigate the dynamic PV models presented in Fig. 2, the relationships between the load current-voltage can be defined via s-domain as given in Eq.(6) [13].

$$i_L(s) = \frac{V_{oc}}{s}\frac{a_{21}(s + b_1) + b_2(s - a_{11})}{(s - a_{22})(s - a_{11}) - a_{12}a_{21}}, \tag{6}$$

where,

$$\begin{pmatrix} a_{11} & a_{12} \\ a_{21} & a_{22} \end{pmatrix} = \begin{pmatrix} \frac{-1}{C(R_c+R_s)} & \frac{-R_s}{C(R_c+R_s)} \\ \frac{R_s}{L(R_c+R_s)} & \frac{-[R_L R_c + R_s R_c + R_L R_s]}{L(R_c+R_s)} \end{pmatrix}, \qquad \begin{pmatrix} b_1 \\ b_2 \end{pmatrix} = \begin{pmatrix} \frac{1}{C(R_s+R_c)} \\ \frac{R_c}{L(R_c+R_s)} \end{pmatrix} \tag{7}$$

From the obtained Eqs. (6) and (7), it can be noticed that the parameters which need to be estimated are R_C, C and L via known parameters of the static part.

3. Problem definitions

The parameter estimation of different PV models is considered a nonlinear optimization problem. It is treated as a decisive task to model an accurate PV model that replicates the efficiency of the entire PV system. To achieve this, an optimization problem designed with an objective function of minimization and it also requires identifying the variables which are involved in it. The effectiveness of the estimated model parameters using optimization techniques is sensitive to the changes that occurred in the implemented objective function. With this objective, in this work, the authors considered the root mean square error (RMSE) among the measured and the estimated current for identifying the static and dynamic PV models' parameters. The mathematical formulas of the objective function based on the static and dynamic models have been documented as follows:

3.1. Problem Formulation: Static models

For the SDM and DDM, the RMSE among the measured and the estimated current using the estimated parameters has been computed as the applied objective function. The estimated current can be figured dependent on the identified parameters with the help of NR function to deal with the nonlinear equations of the PV model as presented as in Eq.(8):

- The objective function :

$$obj(Z) = \sqrt{\frac{1}{M}\sum_{i=1}^{M}\left(I_{meas_i} - I_{est_i}(V_{meas_i}, Z)\right)^2} \tag{8}$$

where I_{est} and I_{meas} indicates the estimated and measured currents, respectively. The I_{est} is evaluated via the estimated parameters and by solving Eq.(1) and 4 adopting NR method as described in Eq.(9):

$$I_{est} = I_{est} - \frac{(dI)}{(dI')} \tag{9}$$

where, dI serves as the difference function of I, dI' is the 1^{st} derivative of dI with respect to I. The respective equations can be given as follows:
For SDM, the functions of dI and dI' can be written as shown in Eq.(10), (11):

$$dI = I_g - I_{o1}\left(exp\left(\frac{(V + IR_s)}{aV_t} - 1\right)\right) - \frac{(V + IR_s)}{R_p} - I. \tag{10}$$

$$dI' = -I_{o1}\frac{R_s}{aV_t}\left(exp\left(\frac{(V + IR_s)}{aV_t} - 1\right)\right) - \frac{(R_s)}{R_p} - 1 \tag{11}$$

By following the similar procedure using mentioned equations I_{est}, dI, and dI' for DDM can also evaluated.

3.1.1. Evaluating the results

To test the superiority of the proposed population-based method, Lambert function is taken into account to estimate the currents of SDM, DDM and PV module. The RMSE has been recomputed based on the estimated current via Lambert W function ($\text{RMSE}_{Lambert}$). The presence of a high difference in RMSE values obtained via Lambert and for Eq.(8) shows the inefficiency of the extracted parameters.

The Lambert functions of SDM and DDM can be given as follows:

- Lambert form for SDM Eq.(1)

$$I_{Lambert} = \frac{Rp\left(I_g + I_{o1} - V\right)}{R_s + R_p} - \frac{a_1 V_t}{R_s} W(\delta), \quad where \tag{12a}$$

$$\delta = \frac{I_{o1} R_p R_s}{a_1 V_t (R_s + R_p)} exp\left(\frac{R_p\left(R_s I_g + R_s I_{o1} + V\right)}{a_1 V_t\left(R_s + R_p\right)}\right), \tag{12b}$$

- Lambert form for DDM Eq.(4).

$$I_{Lambert} = \frac{Rp(I_{oh} + I_{o1} + I_{o2} - V)}{R_s + R_p} - r\frac{a_1 V_t}{R_s} W(\delta_1) - (1-r)\frac{a_2 V_t}{R_s} W(\delta_2), \tag{13a}$$

$$where \tag{13b}$$

$$r = \frac{I_{o1}\left[exp\left(\frac{(V+IR_s)}{a_1 V_t}\right) - 1\right]}{I_{o1}\left[exp\left(\frac{(V+IR_s)}{a_1 V_t}\right) - 1\right] - I_{o2}\left[exp\left(\frac{(V+IR_s)}{a_2 V_t}\right) - 1\right]} \tag{13c}$$

$$\delta_1 = \frac{I_{o1} R_s R_p}{r a_1 V_t (R_s + R_p)} exp\left(\frac{R_p\left(R_s I_g + R_s I_{o1}/r + V\right)}{a_1 V_t\left(R_s + R_p\right)}\right) \tag{13d}$$

$$\delta_2 = \frac{I_{o2} R_s R_p}{(1-r) a_2 V_t (R_s + R_p)} exp\left(\frac{R_p\left(R_s I_g + R_s I_{o2}/(1-r) + V\right)}{a_2 V_t\left(R_s + R_p\right)}\right), \tag{13e}$$

where $I_{Lambert}$ is the evaluated current using Lambert form, W represents solution of Lambert W function. Correspondingly the equation of RMSE can be framed as follow:

$$RMSE_{Lambert} = \sqrt{\frac{1}{M}\sum_{i=1}^{M}\left(I_{meas_i} - I_{Lambert_i}\right)^2} \tag{14}$$

3.2. Problem formulation: Dynamic model

Similar to the SDM and DDM, the RMSE has been recognized as the employed objective function. In it, the unknown parameters are estimated to minimize the difference between the measured dynamic data of the load current and the extracted one using the estimated parameters that can be formulated as in Eq.(15):

$$Obj(Z) = \sqrt{\frac{1}{M}\sum_{i=0}^{M}\left(I_{meas}(t_i) - I_e st(Z, t_i)\right)^2} \tag{15}$$

where M indicates the number of the measured points. Z is the vector of variables (R_C, C, L) and I_{est} and I_{meas} show the estimated and the measured current as functions of time (t_i).

4. Background

4.1. Marine Predators Algorithm (MPA)

Within this section, the necessary steps of the traditional Marine Predators Algorithm (MPA) is introduced [49]. In general, MPA is a meta-heuristic technique which simulates the behaviour of the marine prey and predator in nature.

Similar to other MH techniques, the first step in MPA is to generate a population of N agents/solutions and this performed using the formula in Eq.(16):

$$Z = LB + rand \times (UB - LB) \tag{16}$$

In Eq.(16), $rand$ denotes a random number [0,1]. LB and UB are the the lower and upper boundary of the search domain.

In MPA, there are two matrices named Elite and Prey, which are defined as in Eq.(17):

$$Elite = \begin{bmatrix} Z_{11}^1 & Z_{12}^1 & ... & Z_{1d}^1 \\ Z_{21}^1 & Z_{22}^1 & ... & Z_{2d}^1 \\ ... & ... & ... & ... \\ Z_{n1}^1 & Z_{n2}^1 & ... & Z_{nd}^1 \end{bmatrix}, z = \begin{bmatrix} Z_{11} & Z_{12} & ... & Z_{1d} \\ Z_{21} & Z_{22} & ... & Z_{2d} \\ ... & ... & ... & ... \\ Z_{n1} & Z_{n2} & ... & Z_{nd} \end{bmatrix}, \tag{17}$$

MPA uses three stages to update the solutions, based on the velocity ratio of the predator and prey. The details of these stages are given in the following section.

4.1.1. Stage 1: High-velocity ratio

In this stage, MPA assumed that the prey has high speed, so the movement of the predator should be stopped. This behaviour is performed during the first third from the total number of iterations (i.e., $1/3t_{max}$) and the position of prey is updated using the formula presented in Eq.(18), (19).

$$S_i = R_B \times (Elite_i - R_B \times Z_i), i = 1, 2, ..., n \tag{18}$$

$$Z_i = Z_i + P.R \times S_i,\ P = 0.5 \tag{19}$$

where $R \in [0, 1]$ represents a random vector. R_B denotes the Brownian motion vector.

4.1.2. Stage 2: Unit velocity ratio

In this stage, it is assumed that both prey and predator have the same velocity. This occurred when $\frac{1}{3}t_{max} < t < \frac{2}{3}t_{max}$. The Brownian technique is used to simulate the movement of a predator, whereas the lévy flight is used to emulate the movement of prey.

To update the solutions in this stage, the population is divided into two halves. The solution belongs to the first half are updated using Eqs. (20) and (21) and the solutions in the second half are updated using Eq.(25) and (24).

$$S_i = R_L \times (Elite_i - R_L \times Z_i), \quad i = 1, 2, ..., n/2 \tag{20}$$

$$Z_i = Z_i + P.R \times S_i \tag{21}$$

In Eq.(20), R_L denotes the random number generated from Lévy distribution.

$$S_i = R_B \times (R_B \times Elite_i - Z_i), \quad i = n/2, ..., n \tag{22}$$

$$Z_i = Elite_i + P.CF \times S_i,\ CF = (1 - \frac{t}{t_{max}})^{2\frac{t}{t_{max}})} \tag{23}$$

where, t is the current iteration.

4.1.3. Stage 3: low-velocity ratio

In this stage, it supposes that the prey is slower than predator and that occurred at the last third from the total number of iterations (i.e., $t > \frac{2}{3}t_{max}$). The position is updated using the following formula:

$$Z_i = Elite_i + P.CF \times S_i,\ CF = (1 - \frac{t}{t_{max}})^{2\frac{t}{t_{max}})} \tag{24}$$

$$S_i = R_L \times (R_L \times Elite_i - Z_i), i = 1, 2, ..., n \tag{25}$$

4.1.4. Eddy formation and the effect of FADS

Following [49], the behavioural of predators is changed according to the eddy formation and Fish Aggregating Devices (FADS). This can be formulated using the following equation:

$$Z_i = \begin{cases} Z_i + CF[Z_{min} + R \times (Z_{max} - Z_{min})] \times U & r_5 < FAD \\ Z_i + [FAD(1-r) + r](Z_{r1} - Z_{r2}) & r_5 > FAD \end{cases} \tag{26}$$

where, U is a binary solution. $FAD = 0.2$ and $r \in [0, 1]$. r_1 and r_2 are random index.

4.1.5. Marine memory

In MPA, the marine predator has memory to save the best position. This achieved by comparing the new solution with the saved one and determine the best of them. This updating process is performed at each iteration during the optimization.

4.2. Differential Evolution

In this section, the mathematical definition of the Differential Evolution (DE) [52] is presented. There are steps in DE named crossover, mutation, and selection which make DE is simple, easy to implement, and takes a short time to solve the optimization problem.

In general, DE begins by setting the initial values for N solutions. Followed by computing the fitness value for each solution. Then the solutions are updated using the operators of DE (i.e., mutation, crossover, and selection). The solution Z_i^t is updated using the mutation operator to produce mutation solution Y_i based on the current Z_i as the following equation:

$$Y_i^t = Z_i + F \times (Z_b - Z_i + Z_{rand_1}^t - Z_{rand_2}^t), \tag{27}$$

In Eq.(27), $rand_1$ and $rand_2$, refer to a random indexes varied from 1 to N. F refers to the mutation scaling factor and can be computed using randcaush distribution of the following expression.

$$F = 0.3 + 0.1 * tan(pi * (rand(n, dim) - 0.5)) \tag{28}$$

where, tan is the tangent mathematical function, n number of search agents and dim is the dimension of the considered optimization problem (5 for SDM, 7 for DDM, and 3 for DM)

Followed by using crossover operator to update the solution to be generated, a new solution V_i as in Eq.(29).

$$V_i^t = \begin{cases} Y_i^t & if\ rand \le C_r \\ Z_i^t & otherwise \end{cases} \tag{29}$$

where, $rand \in [0, 1]$ denotes a random value and C_r refers the crossover probability.

The final step is to use the selection operator to update the solution based on either the current solution Z_i or V_i. This achieved according to the value of fitness value:

$$Z_i^{t+1} = \begin{cases} V_i^t & if \ f(V_i^t) < f(Z_i^t) \\ Z_i^t & otherwise \end{cases} \tag{30}$$

These steps of DE (i.e., mutation, crossover, selection) are performed until reached to the terminal criteria.

5. Enhanced marian predator optimizer

The structure of the developed EMPA method is given in Figure 3. The developed EMPA uses the operators of DE to enhance the exploration stage of MPA as it has suitable operators that help to avoid the local point.

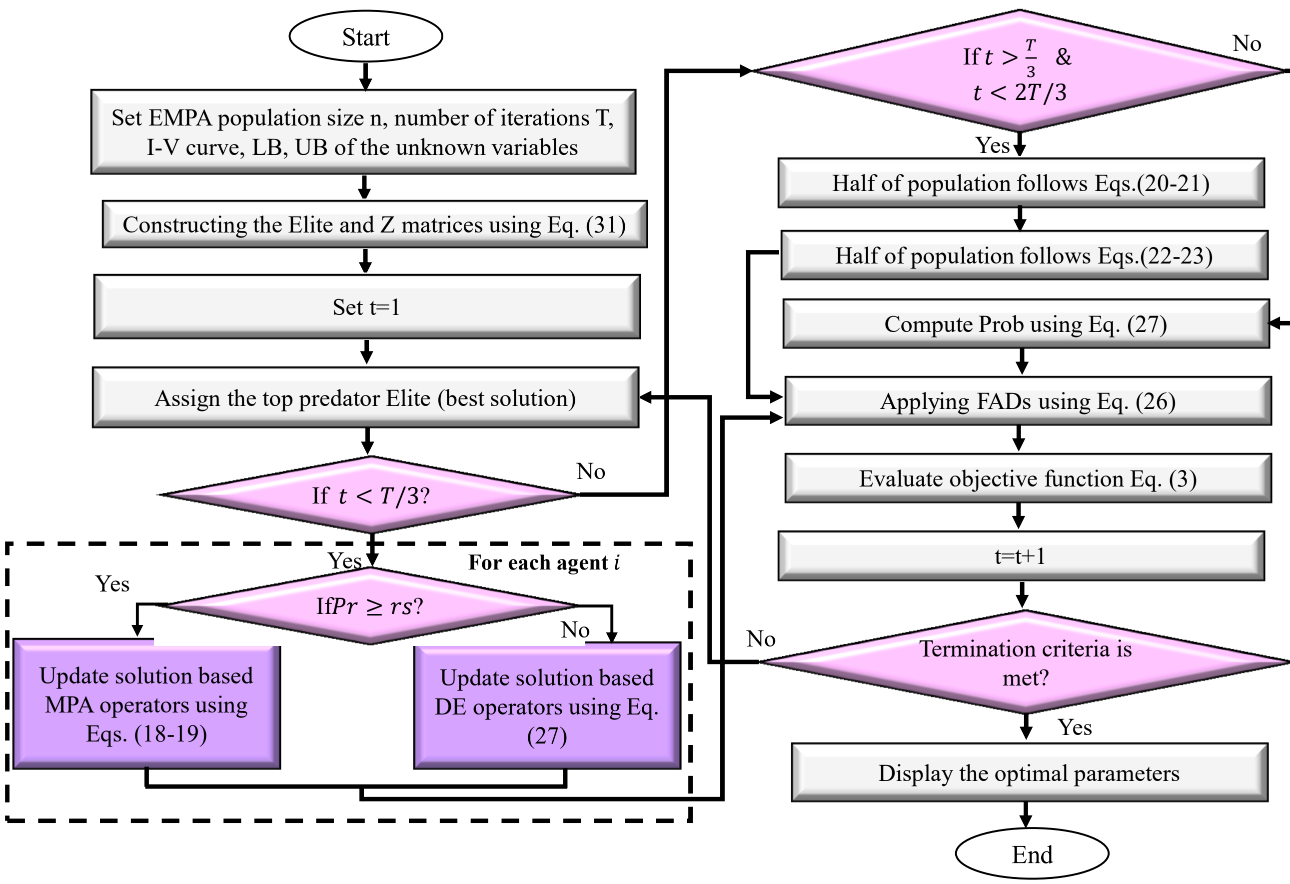

Figure 3: The steps of the EMPA approach.

In general, the developed EMPA starts by using Eq.(31) to generate the initial population Z^{ith}. This performed by using the following equation:

$$Z_{i,j} = LB_j + rand_1 \times (UB_j - LB_j), \ \ j = 1, 2, ..., dim, \ i = 1, 2, ..., N \tag{31}$$

In Eq.(31), the symbols UB_j and LB_j represent the maximum and minimum boundaries at dimension j, respectively.

The process of updating solutions is implemented using the operators of the traditional MPA algorithm supported by DE operator in the exploration phase in (Stage 1) to discover the search space efficiently, and this performed using the following equation.

$$Z_i = \begin{cases} operators\, of\, MPA & Pr_i > r_s \\ operators\, of\, DE & otherwise \end{cases} \tag{32}$$

In Eq.(32), Pr_i is the probability of each X_i and it is formulated as:

$$Pr_i = \frac{Fit_i}{\sum_{i=1}^{N} Fit_i} \tag{33}$$

where

$$r_s = min(Pr_i) + rand \times (max(Pr_i) - min(Pr_i)),\ rand \in [0,1] \tag{34}$$

The main objective of using r_s is to control the process of using the operators of DE and MPA. To avoid the problem of making it a constant value, we update its value according to the probability of each solution. This gives the developed EMPA high flexibility in switching between MPA and DE, as shown in Fig 3.

The next process in EMPE is to process with the second and third stages of the algorithm. Then, the objective function can be evaluated using the current solutions and return by the best solutions (identified model parameters corresponded to a minimum objective function) to generate the Elite matrix. The previously mentioned steps are repeated until the termination condition is met (i.e., here the maximum number of iterations) then the algorithm stops and the best solution vector is displayed.

6. Results and analysis of EMPA

To validate the performance of the proposed method, the EMPA has been tested with several series of experimental data-sets as follows:

1. Series 1: a set of the experimental data of R.T.C solar cell at temperature of 33 $°C$ and irradiation of 1000 W/m^2 has been measured. The length of the data sets is 28 samples. The electric specifications of the cell are I_{sc} = 0.7605 A, V_{oc} = 0.5727 V, I_{mp} = 0.6755 A and V_{mp} = 0.4590 V [24].
2. Series 2: five experimentally measured data-sets for Canadian-Solar-(CS6P-240P) multi-crystalline solar panel at different solar radiations and temperatures that have a profile of 673.5, 580.3, 347.8, 246.65 and 109.2 W/m^2 with 45.92, 51.91, 43.95, 40.05 and 37.32 $°C$, respectively. The used instruments in the measuring process are I-V 400 photovoltaic panel analyzer with HT304N radiating sensor and temperature sensor PT300. The TOPVIEW software was utilized to transfer this data to the personal PC. The electric specifications of the panel at STC are I_{sc} = 8.59 A, V_{oc} = 37 V, I_{mp} = 8.03 A and V_{mp} = 29.9 V.
3. Series 3: dynamic experimental dataset of the load current for the connected PV module with load R_L= 23.1 Ω at an irradiance level of 655 W/m^2 and a temperature of 25 $°C$ has been utilized while identifying the parameters of dynamic PV model. The module is fixed tilted at 50° and the characteristic parameters of the module are V_{oc} = 19.6 V, I_{sc} = 0.96 A, V_{mp} = 14.96 V and I_{mp}= 0.92 A at the irradiance and the temperature levels [32].

The proposed algorithms have been implemented to identify the static models (SDM and DDM), and dynamic one with considering a number of iterations as 500 and population size as 30. The upper and lower boundaries for the studied models are listed in Table 1.

Table 1: The lower and upper boundaries of SDM, DDM and TDM parameters.

R.T.C solar cell (SDM/DDDM)			CS6P-240P solar module (DDM)			Dynamic model		
Parameters	LB	UB	Parameters	LB	UB	Parameters	LB	UB
$R_s(\Omega)$	0	0.5	$R_s(\Omega)$	0	2	$R_c(\Omega)$	0	20
$R_p(\Omega)$	0	1000	$R_p(\Omega)$	0	5000	$C(F)$	$20e^{-9}$	$600e^{-7}$
$I_{pv}(A)$	0	2	$I_{pv}(A)$	0	9	$L(H)$	$5e^{-6}$	$100e^{-6}$
$I_{o1}(\mu A)$	0	2	$I_o(\mu A)$	0	2			
$I_{o2}(\mu A)$	0	2	$I_{o2}(\mu A)$	0	2			
a_1	1	2	a_1	1	2			
a_2	1	2	a_2	1	3			

where LB is lower bounds and UB is the upper boundaries

6.1. Series of experiment 1: R.T.C. France cell

The proposed model has been implemented to extract the unknown parameters for the SDM and DDM at 3 $°C$ and 1000 W/m^2 test conditions for the R.T.C. France cell. Here, several extraction algorithms are utilized to show the superiority of the proposed model. These modes are MPA, fractional chaotic ensemble particle swarm optimizer (EPSO) [33], chaotic heterogeneous comprehensive learning PSO (HCLPSO) [32], performance-guided JAYA (PGJAYA) [27], improved whale optimization algorithm variants (CWOA) and (PSO-WOA) [36], self-adaptive teaching-learning-based optimization (STLBO) [29], enhanced leader particle swarm optimisation (ELPSO)[53], hybrid firefly and pattern search algorithms (HFAPS) [54], multiple learning backtracking search algorithm (MLBSA) [28], time varying acceleration coefficients particle swarm optimisation (TVACPSO) [55], chaos PSO (CPSO) [55], genetic algorithm (GA) [56] , improved cuckoo search algorithm (CSA) and (ICSA) [57]. Accordingly, the extracted parameters based on the proposed model and the other models as well as the statistical comparison between the utilized models are listed in Table 2.

Table 2: The estimated parameters R.T.C. France cell obtained via the proposed approach under different irradiances and temperatures for SDM and DDM.

		Parameters											
Cond/ Mod/Alg		a_1	a_2	$R_s(\Omega)$	$R_p(\Omega)$	$I_{o1}(A)$	$I_{o2}(A)$	$I_{pv}(A)$	RMSE	$RMSE_{lambert}$	$Diff_{RMSE}$	MSAE	AE_{MPP}
SDM	EMPA	1.4771		3.6546e − 02	5.2890e + 01	3.1074e − 07		7.6079e − 01	7.7301e − 04	7.7301e − 04	−9.4376e − 17	6.7820e − 04	4.6006e − 05
	MPA [58]	1.4771		3.6546e − 02	5.2887e + 01	3.1072e − 07		7.6079e − 01	7.7301e − 04	7.7301e − 04	−8.6519e − 17	6.7824e − 04	4.6032e − 05
	EPSO [33]	1.4627		3.7180e − 02	5.637e + 01	2.6887e − 07		7.6075e − 01	8.0621e − 04	8.0671e-04	5.0000e-07		
	HCLPSO [32]	1.4667		3.6995e − 02	5.0678e + 01	2.8002e − 07		7.6083e − 01	7.8958e − 04	7.8959e-04	1.0000e-08		
	PGJAYA[27]	1.4812		3.64e − 02	5.3718e + 01	3.230e − 07		7.608e − 01	9.8602e − 04	9.0444e-04	-8.1580e-05		
	CWOA[36]	1.4821		3.6389e − 02	5.7153e + 01	3.263e − 07		7.6055e − 01	9.9867e − 04	8.5300e-04	-1.4567e-04		
	PSO-WOA[36]	1.4863		3.6124e − 02	5.9323e + 01	3.401e − 07		7.6056e − 01	1.0710e − 03	9.3558e-04	-1.3542e-04		
	STLBO[29]	1.4812		3.638e − 02	5.3725e + 01	3.231e − 07		7.608e − 01	9.8602e − 04	8.7420e-04	-1.1182e-04		
	ELPSO[53]	1.4752		3.6547e − 02	5.2889e + 01	3.106e − 07		7.607e − 01	7.7301e − 04	0.0041	0.0033		
	HFAPS[54]	1.4810		3.6381e − 02	5.3678e + 01	3.226e − 07		7.607e − 01	9.8602e − 04	8.2376e-04	-1.6226e-04		
	MLBSA[28]	1.4812		3.64e − 02	5.3718e + 01	3.230e − 07		7.608e − 01	9.8602e − 04	9.0444e-04	-8.1580e-05		
	TVACPSO[55]	1.4752		3.6547e − 02	5.2889e + 01	3.1068e − 07		7.6078e − 01	7.7301e − 04	0.0040	0.0032		
	CPSO[55]	1.4752		3.6547e − 02	5.2892e + 01	3.106e − 07		7.6078e − 01	7.7301e − 04	0.0040	0.0032		
	GA[56]	1.5701		3.143e − 02	2.9482e + 01	7.4560e − 07		7.6653e − 01	4.1020e − 03	0.0047	5.9800e-04		
	CSA[57]	1.4816		3.6380e − 02	5.3696e + 01	3.2282e − 07		7.6077e − 01	9.8602e − 04	0.0017	7.1398e-04		
	ICSA[57]	1.4817		3.6377e − 02	5.3718e + 01	3.2302e − 07		7.6077e − 01	9.8602e − 04	0.0017	7.1398e − 04		
	IMPA[59]	1.481		3.6377e − 02	5.3718e + 01	3.2302e − 07		7.6077e − 01	9.8602e − 04				
DDM	EMPA	1.411	1.8987	0.037342	55.6225	1.3706e − 07	1e − 06	0.7608	7.4396e − 04	7.6542e − 04	2.1461e − 05	6.5500e − 04	7.2720e − 05
	MPA[58]	1.4011	1.8505	0.037419	55.4579	1.1872e − 07	9.2078e − 07	0.7608	7.4437e − 04	7.6965e − 04	2.5277e − 05	6.5542e − 04	7.5307e − 05
	EPSO [33]	1.4379	1.9032	3.6718e − 02	5.6806e + 01	1.8875e − 07	7.8495e − 07	7.6076e − 01	7.6312e − 04	7.6184e − 04	−1.2800e − 06		
	HCLPSO [32]	1.4593	1.7560	3.6673e − 02	5.3943e + 01	2.4469e − 07	1.8843e − 07	7.6075e − 01	7.6680e − 04	7.7095e − 04	4.1513e − 06		
	PGJAYA [27]	1.4450	2.0000	3.68e − 02	5.5813e + 01	2.103e − 07	8.853e − 07	7.608e − 01	9.8263e − 04	8.6294e − 4	−1.1969e − 04		
	CWOA [36]	1.4498	1.4563	3.7487e − 02	5.0209e + 01	0.0790e − 06	1.669e − 07	7.6063e − 01	1.1300e − 03	9.7657e − 04	−1.5343e − 04		
	PSO-WOA [36]	1.4633	1.7736	3.4223e − 02	8.2822e + 01	2.012e − 07	9.361e − 07	7.6109e − 01	1.6699e − 03	1.4886e − 03	−1.8128e − 04		
	STLBO[29]	1.4598	1.9994	3.663e − 02	5.5117e + 01	2.509e − 07	5.454e − 07	7.6078e − 01	9.8280e − 04	8.6623e − 04	−1.1657e − 04		
	ELPSO[53]	1.8357	1.3860	3.7551e − 02	5.5920e + 01	1e − 6	9.9168e − 8	7.6080e − 01	7.4240e − 04	4.0633e − 03	3.3209e − 03		
	HFAPS[54]	1.4510	2	3.67404e − 02	5.5485e + 01	2.259e − 07	7.493e − 07	7.6078e − 01	9.8248e − 04	8.9867e − 04	−8.3812e − 05		
	MLBSA[28]	1.4515	2	3.67e − 02	5.5461e + 01	2.272e − 07	7.383e − 07	7.608e − 01	9.8249e − 04	9.2984e − 04	−5.2649e − 05		
	GA[56]	1.6087	1.6288	2.9144e − 02	5.1116e + 01	6.6062e − 07	4.5514e − 07	7.6886e − 01	5.9195e − 03	6.1831e − 03	2.6361e − 04		
	CSA[57]	1.9999	1.4616	3.6620e − 02	5.4890e + 01	5.0301e − 07	2.5509e − 07	7.6077e − 01	9.8292e − 04	1.6010e − 03	6.1812e − 04		
	ICSA[57]	1.4515	2.0000	3.6740e − 02	5.5482e + 01	2.2596e − 07	7.4730e − 07	7.6078e − 01	9.8249e − 04	1.6832e − 03	7.0073e − 04		
	IMPA[59]	1.4510	1.9999	3.6740e − 02	5.5485e + 01	2.2597e − 07	7.4934e − 07	7.6078e − 01	9.8248e − 04				

Space in $MSAE$ and AE_{MPP} means it is not available in the main manuscripts.

Based on Table 2, the results show that the proposed model and the MPA model outperform the other extraction models in terms of the RMSE, root mean square error using Lambert form (RMSE$_{lambert}$), the deviation between the obtained fitness function and that via Lambert form (Diff$_{RMSE}$), mean sum absolute error (MSAE), and absolute error at maximum power point (AE_{MPP}) for both SDM and DDM cases. However, the proposed model has a very close accuracy with that obtained by MPA model. Therefore, a more detail comparison is carried out between the proposed and the MPA models in terms of minimum, maximum and mean RMSE, standard deviation (STD) and p-value. The obtained results for this comparison are illustrated in Table 3.

Table 3: Statistical measures for the obtained solutions for DDM of R.T.C. France cell .

		Metrics				EMPA vs MPA		
Algo		Min	Max	Mean	STD	R_+	R_-	p-value
SDM	EMPA	0.00077301	0.00077595	0.00077325	$5.9135e-07$	–	–	–
	MPA	0.00077301	0.00077607	0.00077327	$6.7415e-07$	248	217	0.74987
DDM	EMPA	0.00074396	0.0009213	0.00076936	$3.1849e-05$	-	-	–
	MPA	0.00074437	0.00093679	0.00077685	$4.0102e-05$	292	173	0.22102

From Table 3, it is clear that the proposed model performs better than MPA model in terms of mean RMSE and STD in both SDM and DDM. The proposed model has been achieved a similar value of the minimum RMSE in case of SDM, while the values of the maximum and mean RMSE, as well as the STD, are less than that obtained by the MPA model in SDM and DDM. As a result, the proposed model can be claimed to extract more accurate parameters than MPA and the other aforementioned models.

To visualize the conformity between the actual I-V and P-V curves and the generated curves based on the extracted parameters using the proposed and MPA models, both the I-V and P-V curves are plotted as shown in Figures 4 and 5 for SDM and DDM, respectively. Here, Figures 4(a) and 4(b) shows the experimental I-V and P-V curves, and those generated based on the extracted parameters using the proposed and MPA models in SDM, respectively. At the same time, Figure 4(c) shows the convergence curves for the proposed and MPA models during the 500 iterations in the case of SDM. However, Figures 5(a) and 5(b) shows the experimental I-V and P-V curves, and those generated based on the extracted parameters using the proposed and MPA models in DDM, respectively. Finally, Figure 5(c) shows the convergence curves for the proposed and MPA models during the 500 iterations in the case of DDM.

Based on Figures 4(a) and 4(b) for SDM and Figures 5(a) and 5(b) for DDM, it is clear that the proposed model generates very close I-V and P-V curves in respect to the experimental curves. While Figures 4(c) and 5(c) show that the proposed model converges towards the lower RMSE values faster than MPA model.

6.2. Series of experiment 2: CS6P-240P solar module

To show the effectiveness of the proposed model comparing with MPA model, a second data-set is used. Canadian-Solar-(CS6P-240P) multi-crystalline PV module is utilized in this setup. The solar radiation and temperature values, which are used, can be categorized in five cases as, case 1 ($673.5W/m^2$, 45.92 °C), case 2 ($580.3W/m^2$, 51.91 °C), case 3 ($347.8W/m^2$, 43.95 °C), case 4 ($246.65W/m^2$, 40.05 °C) and case 5 ($109.2W/m^2$, 37.32 °C). Here, the proposed and the MPA models are utilized to extract the unknown parameters in a DDM for these cases. However, four statistical terms are used to compare these two models, namely, RMSE, RMSE$_{lambert}$, Diff$_{RMSE}$, MSAE and AE$_{MPP}$. The extracted parameters as well as statistical comparison between the proposed and MPA models are illustrated in Table 4.

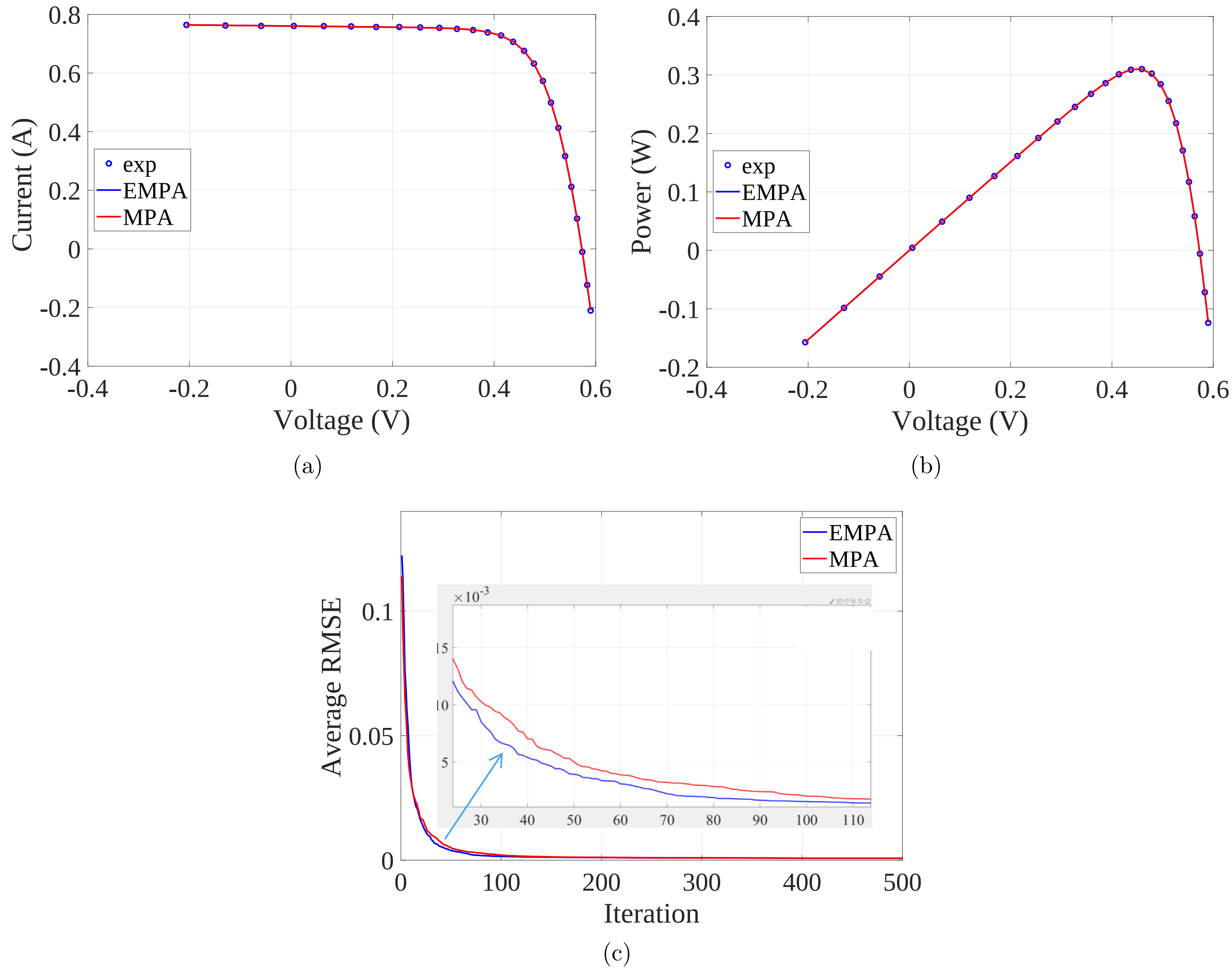

Figure 4: The EMPA and MPA response in case of SDM of R.T.C. France cell in terms of (a) I-V characteristic, (b) P-V characteristic, and (c) Convergence speed.

Table 4: The estimated parameters CS6P-240P solar module by proposed techniques under different irradiance and temperatures for DDM.

		Parameters										
case/Alg		a_1	a_2	$R_s(\Omega)$	$R_p(\Omega)$	$I_{o1}(A)$	$I_{o2}(A)$	$I_{pv}(A)$	RMSE	$RMSE_{lambert}$	$Diff_{RMSE}$	MSAE	AE_{MPP}
# 1	EMPA	1.1651	5	0.31098	328.1285	$1.7414e-07$	$9.9856e-07$	6.9831	0.028491	0.028491	$-1.7352e-08$	0.019330	0.060066
	MPA	1.1663	3.3929	0.31049	318.1901	$1.7729e-07$	$1e-06$	6.985	0.028494	0.028494	$-1.8275e-08$	0.019339	0.094535
# 2	EMPA	1.1594	4.8902	0.31957	890.6115	$2.5923e-07$	$9.6623e-07$	5.9694	0.026738	0.026738	$-9.3975e-09$	0.01717	0.11911
	MPA	1.1593	4.9987	0.31959	896.5043	$2.5908e-07$	$6.9013e-07$	5.9693	0.026738	0.026738	$-6.6834e-09$	0.01718	0.11682
# 3	EMPA	1.1251	4.8846	0.32672	739.0461	$5.318e-08$	$2.2379e-08$	3.0391	0.015227	0.015227	$-6.7708e-10$	0.00686	0.15228
	MPA	1.1203	1.618	0.32153	977.7889	$4.758e-08$	$4.5276e-07$	3.0361	0.015363	0.015353	$-1.0046e-05$	0.00722	0.15338
# 4	EMPA	1.1218	4.9994	0.3594	1294.7382	$3.1325e-08$	$4.8751e-07$	2.1449	0.012647	0.012647	$-3.1356e-09$	0.00607	0.04703
	MPA	1.1426	4.9979	0.33651	1357.1489	$4.352e-08$	$3.3627e-08$	2.145	0.012729	0.012729	$-5.8519e-10$	0.00608	0.11316
# 5	EMPA	1.9904	1	0.73633	449.1236	$5.2695e-09$	$2.2663e-09$	0.99855	0.003561	0.003561	$-2.2048e-08$	0.00218	0.0078932
	MPA	1.0001	1.6309	0.66606	476.8803	$2.1319e-09$	$3.184e-07$	0.99787	0.0036346	0.0036223	$-1.2288e-05$	0.00222	0.049623

From Table 4, the results show that the proposed model has less values of RMSE, $RMSE_{lambert}$, $Diff_{RMSE}$, MSAE and AE_{MPP} in all cases except case 2. In case 2, the values of the RMSE, $RMSE_{lambert}$ are equal for both models, while the values of $Diff_{RMSE}$, MSAE and AE_{MPP} by MPA model are less than those obtained by the proposed model. Therefore, a more detailed comparison is carried out between the proposed model and the MPA model for the same five cases using the

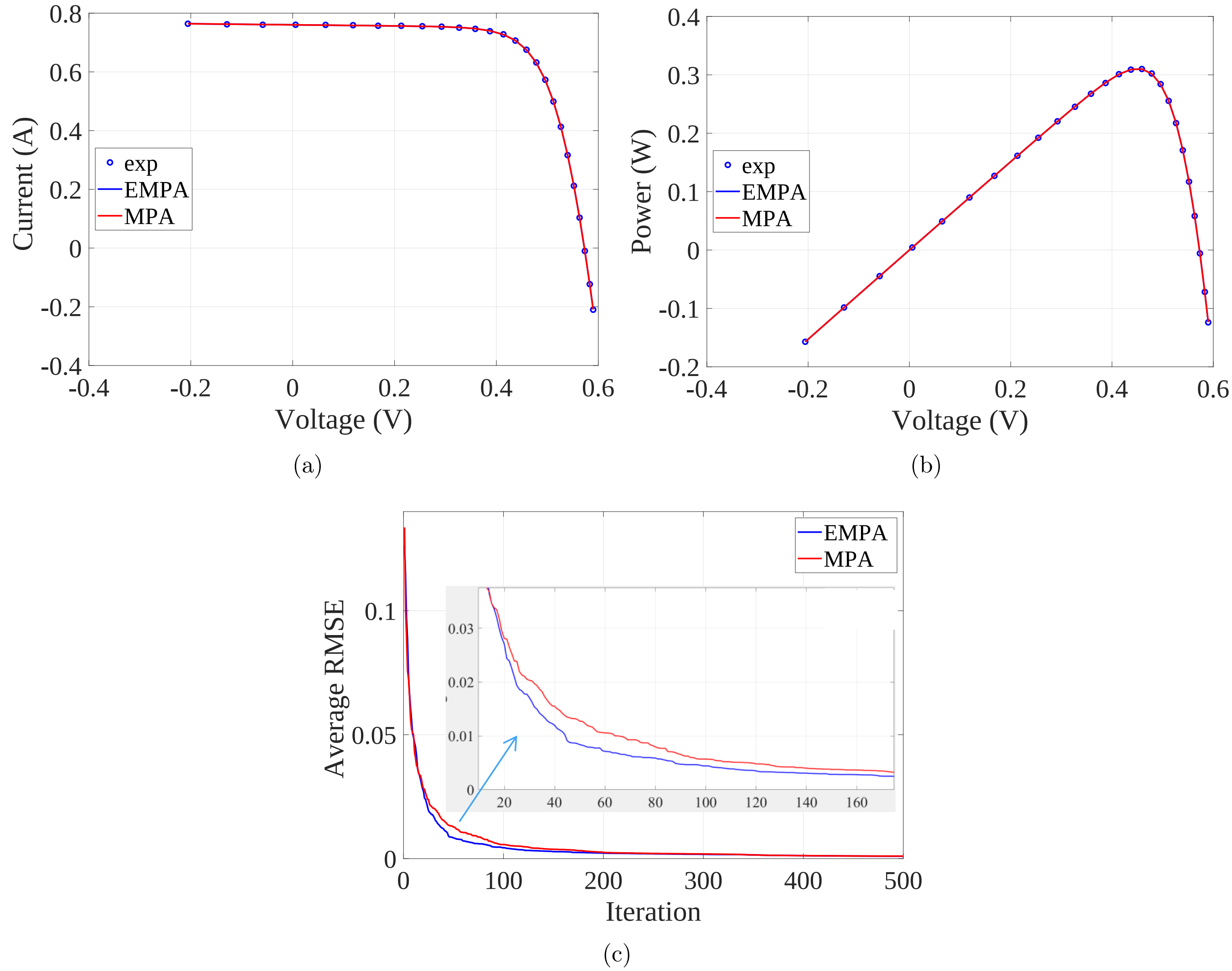

Figure 5: The EMPA and MPA response in case of DDM of RTC france solar cell in terms of (a) I-V characteristic, (b) P-V characteristic, and (c) Convergence speed.

minimum, maximum and mean RMSE, STD and p-value. The results of this comparison are shown in Table 5.

Table 5: Statistical measures for the obtained solutions for DDM of CS6P-240P solar module.

		Metrics				EMPA vs MPA		
Algo		Min	Max	Mean	STD	R_+	R_-	p-value
# 1	EMPA	0.028491	0.02926	0.028763	0.00019427	–	–	–
	MPA	0.028494	0.030495	0.028948	0.00048496	312	152	0.10201
# 2	EMPA	0.026738	0.026898	0.026778	$4.0295e-05$	–	–	–
	MPA	0.026738	0.026972	0.026794	$6.8681e-05$	284	181	0.28948
# 3	EMPA	0.015227	0.016702	0.015866	0.00037802	–	–	–
	MPA	0.015363	0.016491	0.015838	0.00038002	264	201	0.51705
# 4	EMPA	0.012647	0.013817	0.013194	0.0002724	–	–	–
	MPA	0.012729	0.01408	0.013255	0.00030065	266	199	0.4908
# 5	EMPA	0.003561	0.0049799	0.0045914	0.00034021	–	–	–
	MPA	0.0036346	0.0050312	0.0046937	0.00026313	291	174	0.22888

According to Table 5, it is clear that the proposed model outperforms the MPA model for all the cases in terms of minimum, maximum and mean RMSE and STD. It confirms the superiority of the proposed model over the MPA model. To show the effectiveness of the proposed model in generating the I-V and P-V curves, Figure 6 visualizes the generated I-V and P-V curves comparing with the experimental curves as well as the average RMSE curve for the proposed and the MPA models of the CS6P-240P PV model in a DDM. Figure 6(a) and Figure 6(b) show the experimental I-V and P-V curves in the five cases and those generated by the extracted parameters using the proposed and the MPA models, respectively. Moreover, Figure 6(c) shows the average RMSE curves calculated for both models as a difference between the experimental and the generated I-V curves.

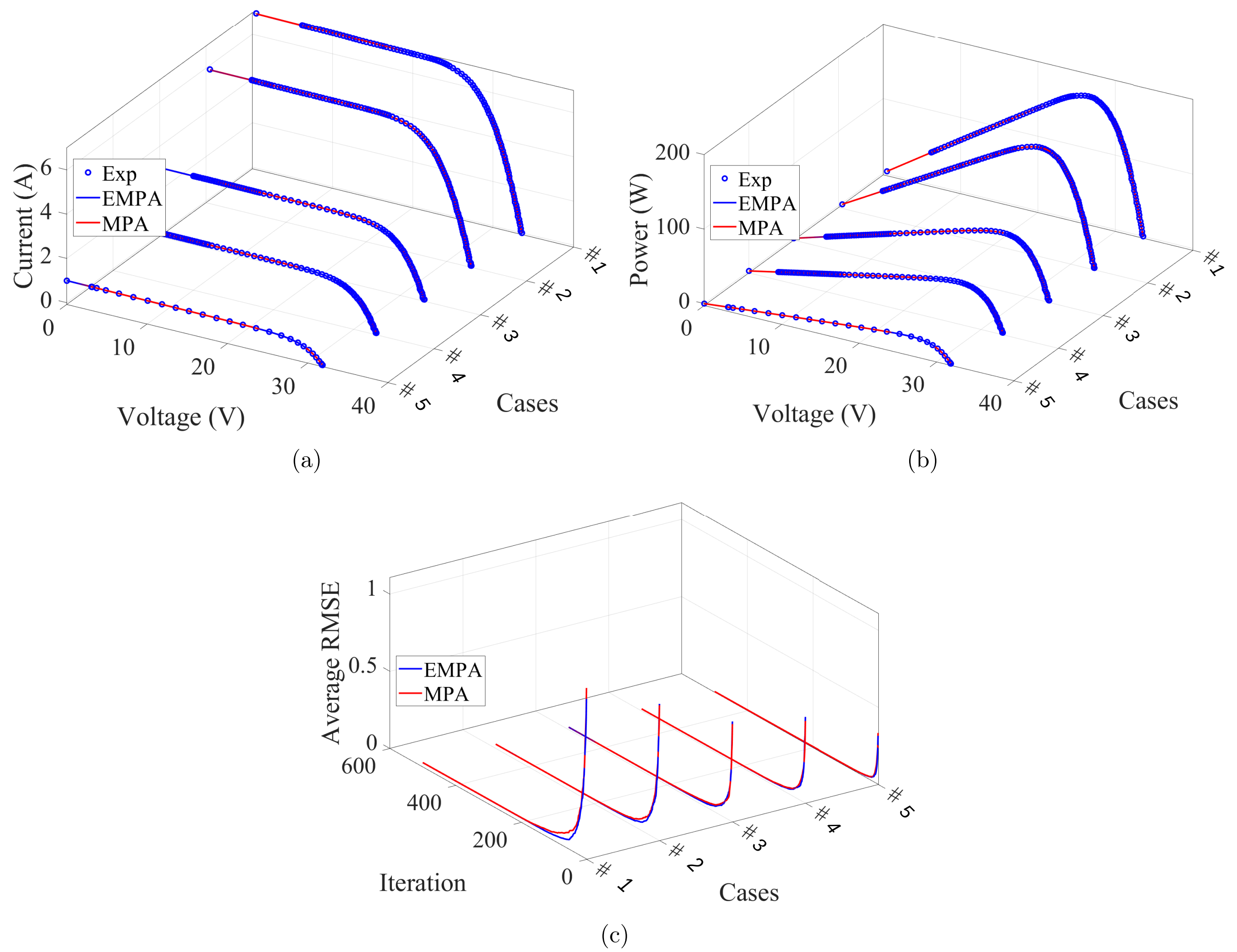

Figure 6: The EMPA and MPA response in case of DDM of CS6P-240P solar module in terms of (a) I-V characteristic, (b) P-V characteristic, and (c) Convergence speed.

From 6(c), it can be noticed that the trends of the average RMSE curves of the proposed model are less than those for the MPA models. That can also graphically claim the better performance that can be obtained by the proposed model to extract the unknown parameters comparing with MPA model.

6.3. Series of experiments 3: dynamic PV model

The proposed model is also validated by extracting the parameters of a dynamic PV model with load R_L= 23.1 Ω. The testing conditions are 655 W/m^2 and 25 $°C$. The proposed model, MPA model and HCLPSO model are used. The optimal extracted parameters, as well as the values of RMSE ± STD are tabulated in Table 6.

Table 6: The estimated parameters of dynamic PV model.

	Parameters			
Alg	$R_c(\Omega)$	C (F)	L (H)	RMSE ± STD
EMPA	7.315	$3.8131e-07$	$7.3251e-06$	$0.0084505 \pm 1.0971e-17$
MPA	7.315	$3.8131e-07$	$7.3251e-06$	$0.0084505 \pm 9.6235e-14$
HCLPSO [32]	7.315	$3.8131e-07$	$7.3251e-06$	$0.0084505 \pm 2.5235e-9$

Based of the values of the RMSE ± STD, the performance of the proposed model is better than those obtained by the MPA and HCLPSO models. To check that visually, the I-T curve for the actual dynamic model as well as the generated curves form the MPA model are illustrated in Figure 7(a). However, Figure 7(b) shows the convergence curves for the proposed and MPA models. From Figure

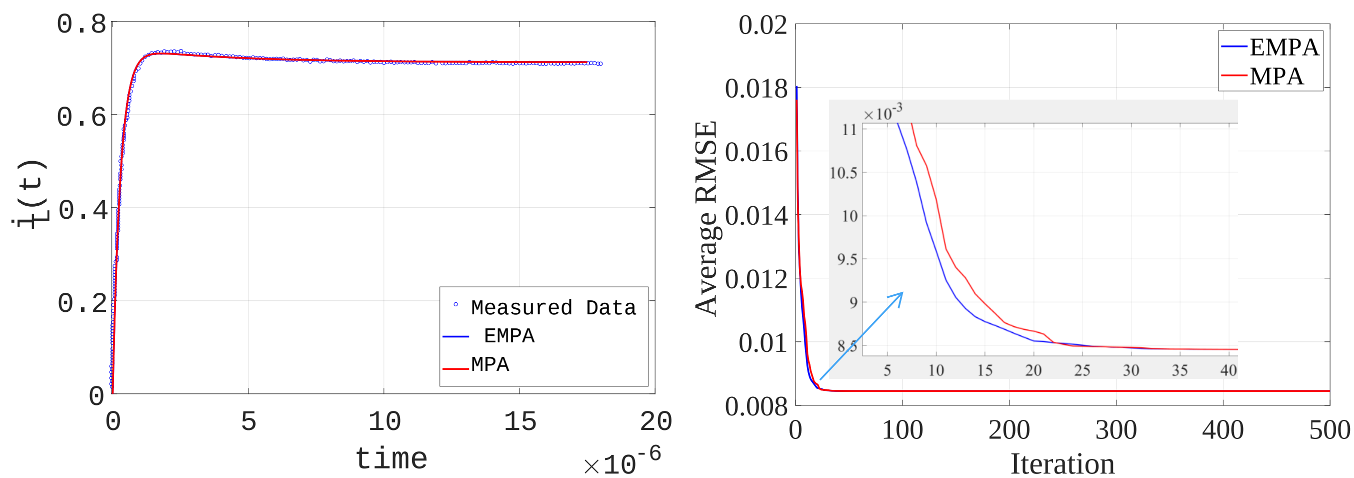

(a) (b)

Figure 7: The EMPA and MPA response in case of dynamic PV model: (a) I-T curves, (b) Convergence curves.

7(a), it can be clearly noticed that the generated I-T curves using the extracted parameters via the proposed and MPA models are very close to the experimental curve. In addition, the convergence speed for the proposed model is faster to reach the lower average RMSE values comparing with MPA algorithm (see Figure 7(b)).

7. Sensitivity analysis

In this section, the sensitivity of the proposed EMPA is evaluated to the variation of the number of iterations, therefore five levels of iteration numbers are implemented (50, 500, 1000, 5000, 10000) iteration. For a brief, the investigation is performed using the first experimental datasets of R.T.C. France cell solar cell while the proposed algorithm extracts the DDM parameters. Table 7 depicts the average of the different measures of EMPA and traditional MPA according to different set of iterations. It can be concluded that the performance in improved with increase the number of iterations. However, it can be noticed that the difference between the results obtained at number of iterations 500, 1000, 5000, and 10000 is small, but the performance of EMPA still better than traditional MPA. The same observation can be noticed from Figure 8.

Table 7: The algorithm performance with changing the iteration numbers.

		Metrics				
Iter	Algo	Min	Max	Mean	STD	execution time (sec)
# 50	EMPA	0.00085798	0.0049628	0.0022956	0.0010498	0.17717
	MPA	0.0012703	0.0035977	0.0022181	0.00058326	0.16188
# 500	EMPA	0.00074396	0.0009213	0.00076936	$3.1849e-05$	1.2526
	MPA	0.00074437	0.00093679	0.00077685	$4.0102e-05$	1.1315
# 1000	EMPA	0.00074724	0.00077288	0.00076008	$7.9447e-06$	2.4884
	MPA	0.00074523	0.00080485	0.00077146	$1.2575e-05$	2.2283
# 5000	EMPA	0.0007422	0.00075649	0.00074363	$2.5292e-06$	13.9049
	MPA	0.00074245	0.000762	0.00074549	$4.5583e-06$	12.4418
# 10000	EMPA	0.00074194	0.00074217	0.00074199	$8.1002e-08$	23.6025
	MPA	0.00074194	0.00074876	0.00074236	$1.2833e-06$	21.8444

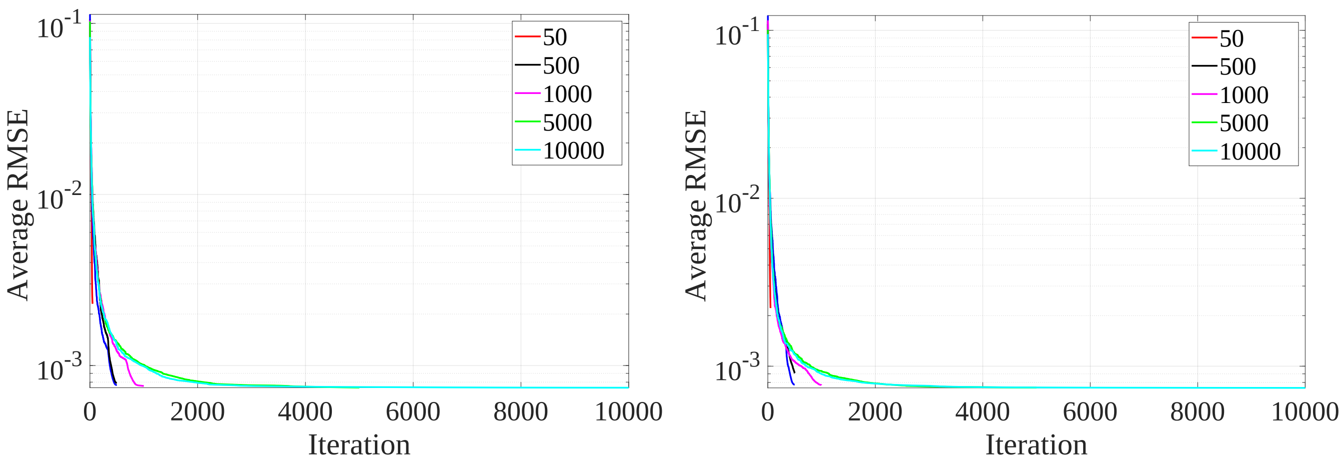

(a) (b)

Figure 8: The mean convergence curves with changing the iteration numbers for (a) EMPA, and (b) MPA.

8. Conclusion

A novel EMPA algorithm was proposed to identify the unknown parameters for several PV models. The proposed algorithm was a developed version of the classical MPA algorithm by applying the concept of the DE algorithm to improve its exploration. The main modification of the proposed EMPA has the following characteristics: (1) sustaining variety in creating new solutions during the search process moderating unanticipated convergence; (2) bypassing the stagnation of the leaders and the sequential population stagnation; (3) consolidating various swarms with several search mechanisms, which allows the logical balance between its exploration and exploitation capabilities; (4) guaranteeing effectiveness and efficiency of the proposed algorithm by adjusting the solutions based on the performance dynamically; and (5) readjusting the optimization problem that being solved and concurrently exploring diverse regions of the multi-dimensional search space. The proposed model is utilized to extract the unknown parameters of two static PV models; a single-diode and a double diode models. In addition, the unknown parameters of a dynamic PV model are identified via the proposed algorithm. Accordingly, three extensive experiments were conducted to evaluate the effectiveness and show the superiority of the proposed model. The proposed performance was compared with those obtained by some recently published algorithms, such as MPA, EPSO, HCLPSO, PGJAYA, CWOA, PSO-WOA, STLBO, ELPSO, HFAPS, MLBSA, TVACPSO, CPSO, GA, CSA, and ICSA. Reflecting on the optimization problems and the mentioned comparisons, the proposed algorithm outperforms the aforementioned algorithms in all case studies for both the static and dynamic PV models. Therefore, the proposed algorithm can be considered as an accurate algorithm for identifying the unknown parameters of the PV models in terms of data fitting, convergence rate, stability and consistency.

References

[1] D. Yousri, T. S. Babu, D. Allam, V. K. Ramachandaramurthy, M. B. Etiba, A novel chaotic flower pollination algorithm for global maximum power point tracking for photovoltaic system under partial shading conditions, IEEE Access 7 (2019) 121432–121445.

[2] http://www.pvresources.com, Pv power plants 2019 global industry guide, http://www.pvresources.com 31 December (2019).

[3] A. Sohani, M. H. Shahverdian, H. Sayyaadi, D. A. Garcia, Impact of absolute and relative humidity on the performance of mono and poly crystalline silicon photovoltaics; applying artificial neural network, Journal of Cleaner Production 276 (2020) 123016.

[4] R. Khezzar, M. Zereg, A. Khezzar, Modeling improvement of the four parameter model for photovoltaic modules, Solar Energy 110 (2014) 452–462.

[5] J. P. Ram, T. S. Babu, T. Dragicevic, N. Rajasekar, A new hybrid bee pollinator flower pollination algorithm for solar pv parameter estimation, Energy conversion and management 135 (2017) 463–476.

[6] D. Alam, D. Yousri, M. Eteiba, Flower pollination algorithm based solar pv parameter estimation, Energy Conversion and Management 101 (2015) 410–422.

[7] T. S. Babu, J. P. Ram, K. Sangeetha, A. Laudani, N. Rajasekar, Parameter extraction of two diode solar pv model using fireworks algorithm, Solar energy 140 (2016) 265–276.

[8] M. Majidi Nezhad, A. Heydari, D. Groppi, F. Cumo, D. Astiaso Garcia, Wind source potential assessment using sentinel 1 satellite and a new forecasting model based on machine learning: A case study sardinia islands, Renewable Energy 155 (2020) 212–224.

[9] E. I. Batzelis, S. A. Papathanassiou, A method for the analytical extraction of the single-diode pv model parameters, IEEE Transactions on Sustainable Energy 7 (2015) 504–512.

[10] T. Ayodele, A. Ogunjuyigbe, E. Ekoh, Evaluation of numerical algorithms used in extracting the parameters of a single-diode photovoltaic model, Sustainable Energy Technologies and Assessments 13 (2016) 51–59.

[11] V. Khanna, B. Das, D. Bisht, P. Singh, et al., A three diode model for industrial solar cells and estimation of solar cell parameters using pso algorithm, Renewable Energy 78 (2015) 105–113.

[12] M. C. Di Piazza, G. Vitale, Photovoltaic sources: modeling and emulation, Springer Science & Business Media, 2012.

[13] M. C. Di Piazza, M. Luna, G. Vitale, Dynamic pv model parameter identification by least-squares regression, IEEE Journal of Photovoltaics 3 (2013) 799–806.

[14] V. J. Chin, Z. Salam, K. Ishaque, Cell modelling and model parameters estimation techniques for photovoltaic simulator application: A review, Applied Energy 154 (2015) 500–519.

[15] A. M. AbdelAty, A. G. Radwan, A. S. Elwakil, C. Psychalinos, Transient and steady-state response of a fractional-order dynamic pv model under different loads, Journal of Circuits, Systems and Computers 27 (2018) 1850023.

[16] D. S. Chan, J. C. Phang, Analytical methods for the extraction of solar-cell single-and double-diode model parameters from iv characteristics, IEEE Transactions on Electron devices 34 (1987) 286–293.

[17] J. Bai, S. Liu, Y. Hao, Z. Zhang, M. Jiang, Y. Zhang, Development of a new compound method to extract the five parameters of pv modules, Energy Conversion and Management 79 (2014) 294–303.

[18] D. Wei, M. Wei, H. Cai, X. Zhang, L. Chen, Parameters extraction method of pv model based on key points of iv curve, Energy Conversion and Management 209 (2020) 112656.

[19] X. Gao, Y. Cui, J. Hu, G. Xu, Y. Yu, Lambert w-function based exact representation for double diode model of solar cells: Comparison on fitness and parameter extraction, Energy conversion and management 127 (2016) 443–460.

[20] W. Long, S. Cai, J. Jiao, M. Xu, T. Wu, A new hybrid algorithm based on grey wolf optimizer and cuckoo search for parameter extraction of solar photovoltaic models, Energy Conversion and Management 203 (2020) 112243.

[21] D. Kler, Y. Goswami, K. Rana, V. Kumar, A novel approach to parameter estimation of photovoltaic systems using hybridized optimizer, Energy Conversion and Management 187 (2019) 486–511.

[22] L. Sandrolini, M. Artioli, U. Reggiani, Numerical method for the extraction of photovoltaic module double-diode model parameters through cluster analysis, Applied Energy 87 (2010) 442–451.

[23] A. Ortiz-Conde, F. J. G. Sánchez, J. Muci, New method to extract the model parameters of solar cells from the explicit analytic solutions of their illuminated i–v characteristics, Solar Energy Materials and Solar Cells 90 (2006) 352–361.

[24] T. Easwarakhanthan, J. Bottin, I. Bouhouch, C. Boutrit, Nonlinear minimization algorithm for determining the solar cell parameters with microcomputers, International journal of solar energy 4 (1986) 1–12.

[25] M. Kumar, A. Kumar, An efficient parameters extraction technique of photovoltaic models for performance assessment, Solar Energy 158 (2017) 192–206.

[26] M. Merchaoui, A. Sakly, M. F. Mimouni, Particle swarm optimisation with adaptive mutation strategy for photovoltaic solar cell/module parameter extraction, Energy conversion and management 175 (2018) 151–163.

[27] K. Yu, B. Qu, C. Yue, S. Ge, X. Chen, J. Liang, A performance-guided jaya algorithm for parameters identification of photovoltaic cell and module, Applied energy 237 (2019) 241–257.

[28] K. Yu, J. Liang, B. Qu, Z. Cheng, H. Wang, Multiple learning backtracking search algorithm for estimating parameters of photovoltaic models, Applied energy 226 (2018) 408–422.

[29] K. Yu, X. Chen, X. Wang, Z. Wang, Parameters identification of photovoltaic models using self-adaptive teaching-learning-based optimization, Energy Conversion and Management 145 (2017) 233–246.

[30] S. Li, W. Gong, X. Yan, C. Hu, D. Bai, L. Wang, L. Gao, Parameter extraction of photovoltaic models using an improved teaching-learning-based optimization, Energy conversion and management 186 (2019) 293–305.

[31] S. Li, Q. Gu, W. Gong, B. Ning, An enhanced adaptive differential evolution algorithm for parameter extraction of photovoltaic models, Energy Conversion and Management 205 (2020) 112443.

[32] D. Yousri, D. Allam, M. Eteiba, P. N. Suganthan, Static and dynamic photovoltaic models' parameters identification using chaotic heterogeneous comprehensive learning particle swarm optimizer variants, Energy conversion and management 182 (2019) 546–563.

[33] D. Yousri, S. B. Thanikanti, D. Allam, V. K. Ramachandaramurthy, M. Eteiba, Fractional chaotic ensemble particle swarm optimizer for identifying the single, double, and three diode photovoltaic models' parameters, Energy 195 (2020) 116979.

[34] M. Premkumar, T. S. Babu, S. Umashankar, R. Sowmya, A new metaphor-less algorithms for the photovoltaic cell parameter estimation, Optik (2020) 164559.

[35] H. M. Hasanien, Performance improvement of photovoltaic power systems using an optimal control strategy based on whale optimization algorithm, Electric Power Systems Research 157 (2018) 168–176.

[36] G. Xiong, J. Zhang, D. Shi, Y. He, Parameter extraction of solar photovoltaic models using an improved whale optimization algorithm, Energy conversion and management 174 (2018) 388–405.

[37] X. Chen, B. Xu, C. Mei, Y. Ding, K. Li, Teaching–learning–based artificial bee colony for solar photovoltaic parameter estimation, Applied energy 212 (2018) 1578–1588.

[38] X. Chen, K. Yu, Hybridizing cuckoo search algorithm with biogeography-based optimization for estimating photovoltaic model parameters, Solar Energy 180 (2019) 192–206.

[39] M. H. Qais, H. M. Hasanien, S. Alghuwainem, Identification of electrical parameters for three-diode photovoltaic model using analytical and sunflower optimization algorithm, Applied Energy 250 (2019) 109–117.

[40] H. Nunes, J. Pombo, S. Mariano, M. Calado, J. F. De Souza, A new high performance method for determining the parameters of pv cells and modules based on guaranteed convergence particle swarm optimization, Applied energy 211 (2018) 774–791.

[41] S. Li, W. Gong, L. Wang, X. Yan, C. Hu, A hybrid adaptive teaching–learning-based optimization and differential evolution for parameter identification of photovoltaic models, Energy Conversion and Management 225 (2020) 113474.

[42] Y. Tao, J. Bai, R. K. Pachauri, A. Sharma, Parameter extraction of photovoltaic modules using a heuristic iterative algorithm, Energy Conversion and Management 224 (2020) 113386.

[43] J. Zhang, Y. Liu, Y. Li, K. Ding, L. Feng, X. Chen, X. Chen, J. Wu, A reinforcement learning based approach for on-line adaptive parameter extraction of photovoltaic array models, Energy Conversion and Management 214 (2020) 112875.

[44] B. Yang, J. Wang, X. Zhang, T. Yu, W. Yao, H. Shu, F. Zeng, L. Sun, Comprehensive overview of meta-heuristic algorithm applications on pv cell parameter identification, Energy Conversion and Management 208 (2020) 112595.

[45] X. Yang, W. Gong, L. Wang, Comparative study on parameter extraction of photovoltaic models via differential evolution, Energy Conversion and Management 201 (2019) 112113.

[46] H. Nunes, P. Silva, J. Pombo, S. Mariano, M. Calado, Multiswarm spiral leader particle swarm optimisation algorithm for pv parameter identification, Energy Conversion and Management 225 (2020) 113388.

[47] M. A. Soliman, H. M. Hasanien, A. Alkuhayli, Marine predators algorithm for parameters identification of triple-diode photovoltaic models, IEEE Access 8 (2020) 155832–155842.

[48] D. Yousri, H. M. Hasanien, A. Fathy, Parameters identification of solid oxide fuel cell for static and dynamic simulation using comprehensive learning dynamic multi-swarm marine predators algorithm, Energy Conversion and Management 228 (2021) 113692.

[49] A. Faramarzi, M. Heidarinejad, S. Mirjalili, A. H. Gandomi, Marine predators algorithm: A nature-inspired metaheuristic, Expert Systems with Applications (2020) 113377.

[50] D. Yousri, T. S. Babu, E. Beshr, M. B. Eteiba, D. Allam, A robust strategy based on marine predators algorithm for large scale photovoltaic array reconfiguration to mitigate the partial shading effect on the performance of pv system, IEEE Access 8 (2020) 112407–112426.

[51] I. A. Ibrahim, M. J. Hossain, B. C. Duck, A. Q. H. Badar, Parameters extraction of a photovoltaic cell model using a co-evolutionary heterogeneous hybrid algorithm, in: 2019 20th International Conference on Intelligent System Application to Power Systems (ISAP), 2019, pp. 1–6. doi:doi:10.1109/ISAP48318.2019.9065989.

[52] R. Storn, K. Price, Differential evolution–a simple and efficient heuristic for global optimization over continuous spaces, Journal of global optimization 11 (1997) 341–359.

[53] A. R. Jordehi, Enhanced leader particle swarm optimisation (elpso): An efficient algorithm for parameter estimation of photovoltaic (pv) cells and modules, Solar Energy 159 (2018) 78–87.

[54] A. M. Beigi, A. Maroosi, Parameter identification for solar cells and module using a hybrid firefly and pattern search algorithms, Solar Energy 171 (2018) 435–446.

[55] A. R. Jordehi, Time varying acceleration coefficients particle swarm optimisation (tvacpso): A new optimisation algorithm for estimating parameters of pv cells and modules, Energy Conversion and Management 129 (2016) 262–274.

[56] A. R. Jordehi, Gravitational search algorithm with linearly decreasing gravitational constant for parameter estimation of photovoltaic cells, in: 2017 IEEE Congress on Evolutionary Computation (CEC), IEEE, 2017, pp. 37–42.

[57] T. Kang, J. Yao, M. Jin, S. Yang, T. Duong, A novel improved cuckoo search algorithm for parameter estimation of photovoltaic (pv) models, Energies 11 (2018) 1060.

[58] D. Yousri, M. Abd Elaziz, D. Oliva, L. Abualigah, M. A. Al-qaness, A. A. Ewees, Reliable applied objective for identifying simple and detailed photovoltaic models using modern metaheuristics: Comparative study, Energy Conversion and Management 223 (2020) 113279.

[59] M. Abdel-Basset, D. El-Shahat, R. K. Chakrabortty, M. Ryan, Parameter estimation of photovoltaic models using an improved marine predators algorithm, Energy Conversion and Management 227 (2021) 113491.